Characterization of Human DHRS6, an Orphan Short Chain Dehydrogenase/Reductase Enzyme

A NOVEL, CYTOSOLIC TYPE 2 R-β-HYDROXYBUTYRATE DEHYDROGENASE*

Received for publication, October 19, 2005, and in revised form, December 23, 2005 Published, JBC Papers in Press, December 27, 2005, DOI 10.1074/jbc.M511346200

Kunde Guo[‡], Petra Lukacik[‡], Evangelos Papagrigoriou[‡], Marc Meier[§], Wen Hwa Lee[‡], Jerzy Adamski[§], and Udo Oppermann^{‡1}

From the ‡ Structural Genomics Consortium, University of Oxford, Oxford OX3 7LD, United Kingdom and the § GSF National Research Center, Institute for Experimental Genetics, 85764 Neuherberg, Germany

Human DHRS6 is a previously uncharacterized member of the short chain dehydrogenases/reductase family and displays significant homologies to bacterial hydroxybutyrate dehydrogenases. Substrate screening reveals sole NAD+-dependent conversion of (R)-hydroxybutyrate to acetoacetate with K_m values of about 10 mM, consistent with plasma levels of circulating ketone bodies in situations of starvation or ketoacidosis. The structure of human DHRS6 was determined at a resolution of 1.8 Å in complex with NAD(H) and reveals a tetrameric organization with a short chain dehydrogenases/reductase-typical folding pattern. A highly conserved triad of Arg residues ("triple R" motif consisting of Arg144, Arg188, and Arg²⁰⁵) was found to bind a sulfate molecule at the active site. Docking analysis of R- β -hydroxybutyrate into the active site reveals an experimentally consistent model of substrate carboxylate binding and catalytically competent orientation. GFP reporter gene analysis reveals a cytosolic localization upon transfection into mammalian cells. These data establish DHRS6 as a novel, cytosolic type 2 (R)hydroxybutyrate dehydrogenase, distinct from its well characterized mitochondrial type 1 counterpart. The properties determined for DHRS6 suggest a possible physiological role in cytosolic ketone body utilization, either as a secondary system for energy supply in starvation or to generate precursors for lipid and sterol synthesis.

Hepatic ketone body formation and utilization of these compounds by peripheral tissues with high energy demands is essential in humans and other mammals for survival during times of starvation and extended fasting. The compounds categorized as ketone bodies comprise acetoacetate, R- β -hydroxybutyrate, and acetone, the last being a nonmetabolizable decarboxylation product of acetoacetate. The liver produces and excretes ketone bodies during times when the amount of acetyl-CoA exceeds the oxidative capacity of hepatic mitochondria. Ketone body formation is thus necessary to maintain β -oxidation by supplying free CoA. This metabolic situation occurs when high amounts of fatty acids derived from peripheral tissues during starvation or fasting are oxidized by β -oxidation pathways. In exacerbated disease states, such as ketoacidotic coma, extremely high amounts of fatty acids are oxidized as a consequence of insulin resistance in diabetes mellitus. In this situation, a potentially life-threatening metabolic acidosis occurs through the high amounts of protons provided by acetoacetate and R-\beta-hydroxybutyrate, exceeding the serum bicarbonate buffer capacity. Serum levels of 5-10 mm ketone bodies are reached under these circumstances as compared with levels of 1 mm in normal states. The liver synthesizes acetoacetate through the enzymes thiolase, hydroxymethylglutaryl-CoA synthase, and hydroxymethylglutaryl-CoA lyase from three molecules of acetyl-CoA, thus producing 1 mol of acetoacetate, 1 mol of acetyl-CoA, and 2 mol of free CoA. Acetoacetate is further reduced to R- β -hydroxybutyrate through mitochondrial *R-β*-hydroxybutyrate dehydrogenase, driven by high levels of NADH in hepatic mitochondria. Peripheral tissues take up ketone bodies and oxidize (R)-hydroxybutyrate back to acetoacetate, which is then ultimately converted into acetyl-CoA entering the tricarboxylic acid cycle.

Mitochondrial R- β -hydroxybutyrate dehydrogenase (BDH)² has been extensively studied (1-5) and constitutes a paradigm of lipid regulation of enzymatic function; however, a crystallographic structural characterization has not been achieved to date. The enzyme belongs to the short chain dehydrogenase/reductase superfamily (6-8), an evolutionarily conserved family of oxidoreductases found in all forms of life. At present, well over 4000 members are deposited in sequence databases, and about 50 three-dimensional structures comprising 20-30 distinct enzymatic activities are available (6-8). Within the human genome, we have previously identified about 70 members of this superfamily (7, 9). Of these human genes, about one-third are still functionally largely uncharacterized, and about 15 human members have been structurally determined. Here we describe the functional and structural annotation of human DHRS6 as a novel, cytosolic type II R-β-hydroxybutyrate dehydrogenase. Human DHRS6 or any other species ortholog represents a previously completely uncharacterized member of the SDR family. The human DHRS6 gene and a putative pseudogene with 95% amino acid sequence identity (DHRS6L) are found on chromosomes 4q24 and 6q16.3, respectively. Human DHRS6 and its vertebrate orthologs show high levels of sequence identities to bacterial hydroxybutyrate dehydrogenases (30 - 40%) (Fig. 1, A and B). This level is higher than that of any other human paralog SDR (30%). Furthermore, a phylogenetic analysis (Fig. 1B) establishes a clear relationship between prokaryotic BDHs and the vertebrate DHRS6 cluster. This finding prompted us to investigate the possibility that DHRS6 acts as hydroxybutyrate dehydrogenase.



^{*} The Structural Genomics Consortium is a registered charity (number 1097737) funded by the Wellcome Trust, GlaxoSmithKline, Genome Canada, the Canadian Institutes of Health Research, the Ontario Innovation Trust, the Ontario Research and Development Challenge Fund, and the Canadian Foundation for Innovation. The costs of publication of this article were defrayed in part by the payment of page charges. This article must therefore be hereby marked "advertisement" in accordance with 18 U.S.C. Section 1734 solely to indicate this fact.

The atomic coordinates and structure factors (code 2AG5) have been deposited in the Protein Data Bank, Research Collaboratory for Structural Bioinformatics, Rutgers University, New Brunswick, NJ (http://www.rcsb.org/).

¹ To whom correspondence should be addressed. E-mail: Udo.Oppermann@ sgc.ox.ac.uk.

² The abbreviations used are: BDH, mitochondrial (R)-hydroxybutyrate dehydrogenase; SDR, short chain dehydrogenase/reductase; MES, 4-morpholineethanesulfonic acid; GFP, green fluorescent protein.

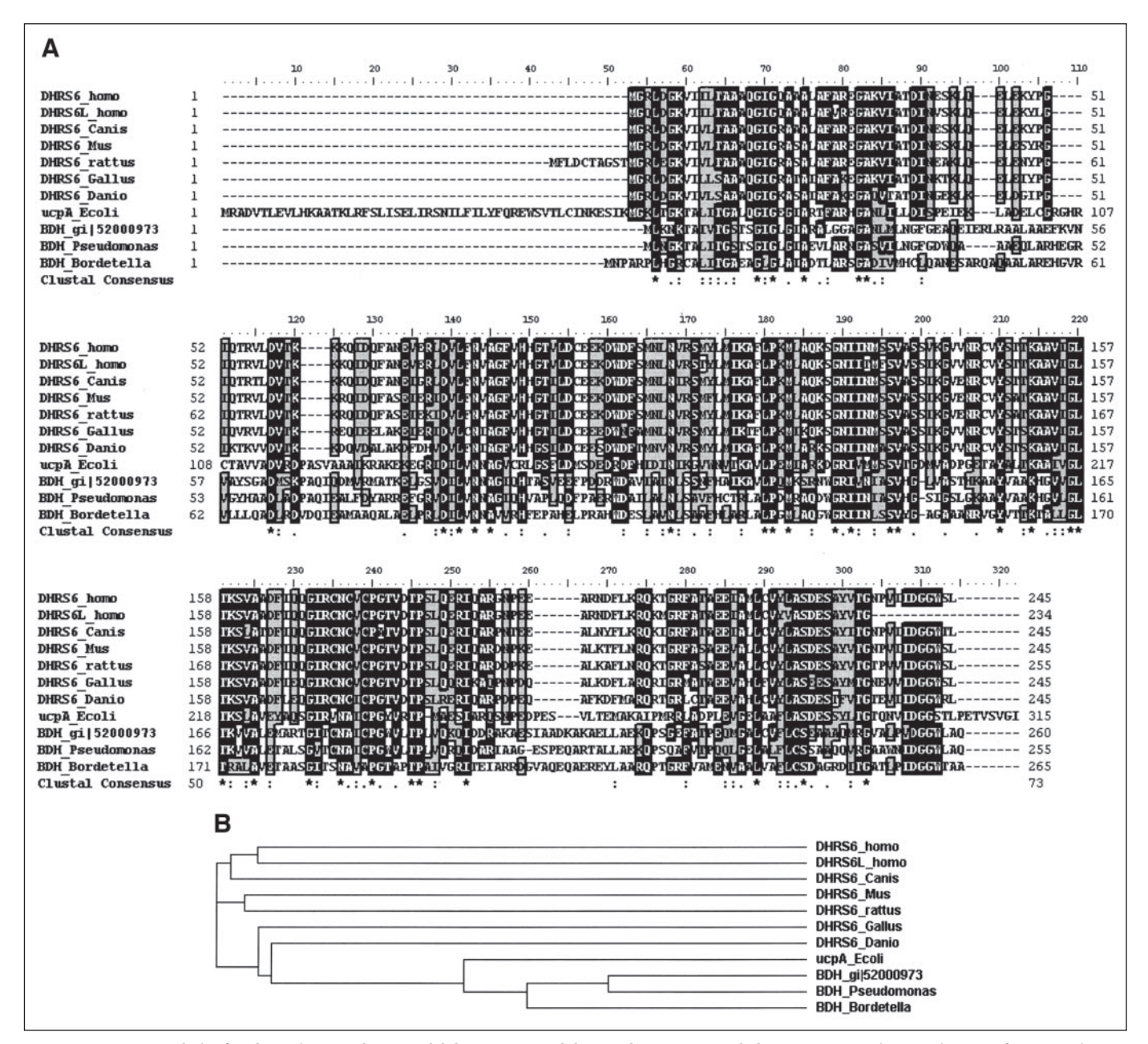


FIGURE 1. Sequence analysis of prokaryotic (R)-OH butyrate dehdyrogenases and the vertebrate DHRS6 orthologs. A, sequence alignment between (from top to bottom) human DHRS6 (DHRS6_homo), human DHRS6L (DHRS6L_homo), canine DHRS6 (DHRS6_canis), murine DHRS6 (DHRS6_mus), rat DHRS6 (DHRS6_rattus), avian DHRS6 (DHRS6_gallus), zebrafish DHRS6 (DHRS6_danio), ucpa from E. coli (ucpa_Ecoli), hydroxybutyrate dehydrogenase from an unspecified culture (BDH_gi|5200973), BDH from Pseudomonas sp. $gi | 8453202| \ (BDH_Pseudomonas), and BDH from \textit{Bordetella bronchiseptica} \ gi | 33603047| \ (BDH_Bordetella). \ Residues involved in catalysis in SDRs and discussed in the text are indicated and the sum of the sum$ by an asterisk, and the conserved triad of Arg residues (triple R motif) is indicated by a double asterisk above the sequences. The figure was created using the program BioEdit. B, cladogram of the sequences given in A.

EXPERIMENTAL PROCEDURES

Cloning, Expression, and Purification of Human DHRS6 and DHRS6L— N-terminally His6-tagged variants encoding human DHRS6 and DHRS6L constructs were expressed in the Escherichia coli expression strain BL21(DE3) in TB medium. For bacterial expression, the coding sequences for human DHRS6 (gi|14754051) and DHRS6L (gi|14754051) were codon-optimized for expression in E. coli. The genes were synthesized (Genscript) and subcloned into a modified pET vector using NdeI and BamHI sites, resulting in an N-terminal His, tag and an engineered TEV protease site and a C-terminal sequence of Gly-Ser before the stop codon. High level soluble protein production was achieved by isopropyl 1-thio- β -D-galactopyranoside induction (0.5 mm) at 18 °C for 12 h.

Whereas expression of soluble DHRS6 was observed, soluble DHRS6L expression proved to be unsuccessful. Cells from DHRS6 cultures were disrupted in a high pressure homogenizer, and the resulting cell lysate was centrifuged for 40 min at 15,000 \times g. The clarified supernatant was then subjected to immobilized metal affinity chromatography (Ni²⁺nitrilotriacetic acid resin; Qiagen) and eluted in 250 mM imidazole, 500 mm NaCl, 50 mm HEPES, pH 7.5, 5% glycerol. This was followed by a final gel filtration chromatographic step on a Superdex 200 HiLoad 26/60 column (GE Healthcare, Uppsala, Sweden). DHRS6 was purified in 10 mm HEPES, pH 7.5, containing 2 mm tris(2-carboxyethyl)phosphine, 5% (w/v) glycerol, and concentrated to 18.3 mg/ml using a 30,000-kDa molecular mass cut-off Amicon Ultra concentration device

(Millipore Corp., Bedford, MA). This two-step purification resulted in a homogenous protein preparation (Fig. 2). The experimentally determined mass by electrospray ionization-time-of-flight mass spectrometry (Agilent LC-MSD TOF) was in agreement with the predicted mass

Crystallization of Human DHRS6—Immediately prior to crystallization, 5 mm NADH (Sigma) was added to the concentrated DHRS6 protein. 50 nl of the protein (at 18.3 mg/ml) was mixed with 100 nl of crystallization solution containing 30% polyethylene glycol monomethylether 5000, 0.2 M ammonium sulfate, and 0.1 M MES, pH 6.5 (Molecular Dimensions Screen I). The crystals were obtained by using the sitting drop vapor diffusion technique at 20 °C.

Data Collection, Processing, and Refinement—A single crystal was transferred to a cryoprotectant consisting of mother liquor and supplemented to a final glycerol concentration of 20% and then flash-frozen in liquid nitrogen. A data set extending to a resolution of 1.84 Å was collected from this crystal on an R-AXIS HTC imaging plate area detector mounted on a Rigaku F-RE SuperBright rotating anode generator (both from Rigaku MSC) operating at 45 kV and 45 mA. Data were indexed, integrated, and scaled using the programs MOSFLM version 6.2.5 and SCALA version 5.0.

Initial phases were calculated by molecular replacement implemented by Phaser version 1.3.1. The search model was an SDR structure with the Protein Data Bank code 1NFF (product of the Rv2002 gene from Mycobacterium tuberculosis). The first maps were of sufficient quality to allow the deletion of incorrect regions and adjustment of the amino acid sequence to the DHRS6 sequence. Starting from this model, 50 cycles of automated model building were carried out using the program ARP/wARP. Water molecules were automatically picked by ARP/ wARP and later checked manually for appropriate density and hydrogen-bonding pattern. The final rounds of manual model building and refinement were carried out in Coot and REFMAC version 5.02.0005, respectively.

Docking Analysis of DHRS6—A molecular three-dimensional model of the substrate molecule (R)-3-hydroxybutyrate was generated using the Dundee PRODRG2 server (available on the World Wide Web at davapc1.bioch.dundee.ac.uk/programs/prodrg/) and saved in the Protein Data Bank format. This molecule and the structure of DHRS6 were loaded into the program ICM (available on the World Wide Web at www.molsoft.com) (10) and converted into the internal coordinates format that includes the addition of hydrogen atoms to the protein model. Both molecules were submitted to the small molecules docking protocol, using pseudoenergy grid potentials to represent the protein molecule and fully flexible ligand molecule as described (10) and implemented in ICM. The active site pocket was easily identified and consisted of a closed cavity inaccessible to the solvent located at the nicotinamide ring end of the bound cofactor molecule. The χ -1 angle of Ser¹³³ was modified to bring the active site to the probable catalytic conformation. The thoroughness parameter was set to 10. The resulting poses of the ligand after docking were individually analyzed.

Substrate Screening and Determination of Kinetic Constants-Enzyme activities were measured as NAD(P)(H)-dependent hydroxydehydrogenase activities of various hydroxybutyryl derivatives. Nucleotide cofactors and D/L-hydroxybutyryl-CoA were from Sigma, and R and S isomers of hydroxybutyrate and hydroxyisobutyrate were obtained from Fluka. Activities were determined by the change of absorbance at 340 nm, using a molar extinction coefficient for NAD(P)H of 6220 M⁻¹ cm⁻¹. Recordings were carried out with a SpectraMax2 (Amersham Biosciences) instrument. Reactions were performed in 1.0-ml volumes or in 96-well microtiter plates in 200-µl volumes at differ-

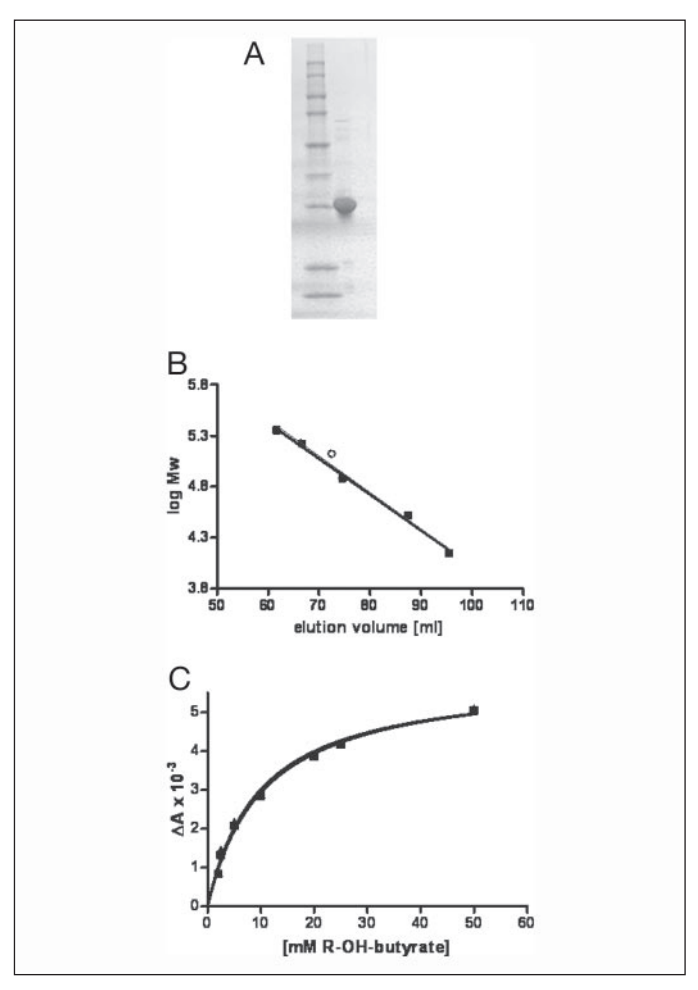


FIGURE 2. Purification and biochemical analysis of human DHRS6. A, SDS-PAGE of recombinant purified human DHRS6. B, tetrameric solution state of DHRS6 determined by gel filtration. Elution volume of recombinant DHRS6 was compared with standard proteins on Superdex S200 columns, and the position of DHRS6 is indicated by an open sphere. The molecular mass was calculated to be 117.3 kDa. C, Michaelis-Menten kinetics of human DHRS6 with NAD+ (1 mm) and varied concentrations of (R)-OH butyrate as substrate, measured at pH 9.0.

ent temperatures and pH values. A linear relationship between product formation and reaction time or amount of enzyme was established and used in subsequent experiments. For determination of kinetic parameters, the substrate concentrations were varied at least between 20 and 500% of an estimated K_m value. Kinetic constants were calculated from initial velocity data by direct curve fitting to the Michaelis-Menten equation ($V = V_{\text{max}} \times S^h / (K_m^h + S^h)$; h = 1) using nonlinear regression analysis and the Prism software package (GraphPad).

Subcellular Localization of Human DHRS6—For localization studies, the full-length coding sequence of human DHRS6 was cloned into different Living Colors™ Vectors (BD Biosciences Clontech, Heidelberg, Germany), resulting in fluorescent protein-tagged constructs. N-terminal green fluorescent protein (GFP) tags were achieved by subcloning into pEGFP-C2; C-terminal tags were constructed by cloning into pAcGFP1-N1. Primers used for amplification of DHRS6 for subcloning into GFP expression vectors were as follows: pEGFP-C2/DHRS6for (TATAGAATTCATGGGTCGACTTGATGGGAAAGTCATC), pEGFP-C2/DHRS6-rev (TTAAGGATCCTCACAAGCTCCAGCCT-CCATCAATG), pAcGFP1-N1/DHRS6-for (TATAAAGCTTATGGG-TCGACTTGATGGGAAAGTCATC), and pAcGFP1-N1/DHRS6-rev (TTAACCGCGGCAAGCTCCAGCCTCCATCAATGATG). Gener-



TABLE 1Kinetic analysis for human DHRS6

Experiments were carried out in the indicated buffer system at saturating concentrations for the second substrate ((R)-OH butyrate (50 mm) or NAD⁺ (1 mm), respectively). Screening experiments for activities with (S)-OH butyrate, DL-OH-butyryl-CoA, and NADP⁺ were carried out at 1 mm NADP⁺, 50 mm (S)-OH-butyrate, and 125 mm DL-OH-butyryl-CoA, respectively, at pH 9.0. NA, no activity detectable. Number of experiments (n) = 4–6. Experiments were carried out at 25 °C unless otherwise stated.

Substrate	Buffer/pH	K_m	$V_{ m max}$	k_{cat}	$k_{\rm cat}/K_m$
		тм	$nmol \times min^{-1} \times mg^{-1}$	min^{-1}	$min^{-1} \times m_M^{-1}$
(R)-OH butyrate	50 mм HEPES, pH 7.5	12.6 ± 5.5	31.9 ± 5.6	0.95 ± 0.2	0.075
(R)-OH butyrate	50 mм Tris/Cl, pH 9.0	10.5 ± 0.7	64.1 ± 2.9	1.9 ± 0.1	0.18
(R)-OH butyrate ^a	50 mм Tris/Cl, pH 9.0	9.1 ± 0.4	82.3 ± 4.3	2.4 ± 0.2	0.26
NAD ⁺	50 mм Tris/Cl, pH 9.0	59.8 ± 11.0	57.0 ± 4.1		
(S)-OH butyrate	50 mм Tris/Cl, pH 9.0	NA			
DL-OH-butyryl-CoA	50 mм Tris/Cl, pH 9.0	NA			
3-OH-R-2-methylbutyrate	50 mм Tris/Cl, pH 9.0	NA			
3-OH-S-2-methylbutyrate	50 mм Tris/Cl, pH 9.0	NA			
NADP ⁺	50 mм Tris/Cl, pH 9.0	NA			

^a Conducted at 30 °C.

TABLE 2Data collection and refinement statistics for DHRS6 crysta

Data collection and refinement statistics for DHRS6 crystal				
Parameters	Values			
Data processing				
Wavelength (Å)	1.54			
Space group	P_1			
Unit cell parameters (Å)	62.1, 62.1, 74.0, 106.0, 106.0, 101.0			
Resolution range (outer shell)(Å)	66.7-1.84 (1.94-1.84)			
Observed reflections (outer shell)	150,655 (15,097)			
Unique reflections (outer shell)	76,179 (7831)			
Completeness (outer shell)(%)	89.7 (62.9)			
Mean $I/\sigma(I)$ (outer shell)	11.8 (3.1)			
Multiplicity (outer shell)	2.0 (1.9)			
$R_{\rm merge}$ (outer shell)	0.062 (0.205)			
V_M (Å 3 Da $^{-1}$)	2.2			
Refinement				
Protein atoms	7449			
Protein residues (per chain)	A, 1–246; B, 2–246; C, 2–245; D, 2–245			
Waters in model	869			
Heteroatoms in model	$4 SO_{4}^{a} 4 NAD$			
R_{work}	0.168			
$R_{ m free}$	0.224			
Root mean square deviation bond lengths (Å)	0.022			
Root mean square deviation bond angles (degrees)	1.744			
Average B factor (Å ²)				
Main chain (per chain)	A:28.6, B:28.7, C:28.6, D:28.6			
Side chain (per chain)	A:31.1, B:30.9, C:30.9, D:30.9			
Waters	37.1			
Ligands	26.8			
Protein Data Bank code	2AG5			
4.60	· · · · · · · · · · · · · · · · · · ·			

 $[^]a$ SO₄, sulfate.

ated constructs were subsequently verified by sequencing on an ABI 3730 DNA analyzer (Applied Biosystems, Foster City, CA).

The human cell line HeLa was maintained in minimal essential medium, 10% fetal bovine serum, 1% penicillin/streptomycin (Invitrogen) at 37 °C and 5% CO $_2$. About 5 \times 10 4 HeLa cells were plated out in 6-well plates containing glass coverslips, transiently transfected with 1 μg of DNA, 3 μl of FuGENE 6 Transfection Reagent (Roche Applied Science) according to the manufacturer's protocol, and studied after an incubation time of 24 h.

For staining of endoplasmic reticulum or mitochondria, cells were incubated under growth conditions for 30 min with fresh medium containing 1 μ M ER-Tracker Blue-White DPX or 300 nM Mito Tracker Orange CMTMRos (stains by Molecular Probes, Karlsruhe, Germany), respectively. Cells were washed twice with PBS and fixed for fluorescence microscopy by incubation for 10 min at growth conditions in medium containing 3.7% formaldehyde. For staining the nucleus, fixed cells were incubated for 2 min under growth conditions with fresh medium containing 300 nM 4',6-diamidino-2-phenylindole solution (in

 $\rm H_2O$; stain by Sigma). Cells were washed twice in PBS, mounted on slides with VectaShield mounting medium (VectorLabs, Grünberg, Germany), and examined with an Axiophot epifluorescence microscope (Zeiss) using a \times 40 oil immersion objective. Three-channel optical data were collected with an ISIS system (Metasystems, Altlussheim, Germany).

RESULTS

Expression, Purification, and Substrate Analysis of Human DHRS6—Whereas human DHRS6 could be expressed and purified in a rapid two-step chromatography procedure (Fig. 2A), yielding about 20 mg of soluble protein per liter of culture, the DHRS6L protein could not be expressed solubly. Gel filtration experiments show that the DHRS6 protein fraction elutes at a position indicating that its solution state is tetrameric (Fig. 2B).

A substrate screening using a spectrophotometric assay with a variety of hydroxybutyryl derivatives reveals that the purified enzyme is active toward (R)- β -hydroxybutyrate but not toward the S enantiomer or toward the (R)- or (S)-hydroxybutyryl-CoA derivatives or toward (S)- or (R)-hydroxyisobutyrate (Table 1). Steady-state kinetic experiments show that R- β -hydroxybutyrate is oxidized with a $V_{\rm max}$ of about 82.3 nmol \times min $^{-1}$ \times mg $^{-1}$ and a K_m of 9.1 mM (Table 1) at 30 °C and at pH 9.0. At pH 7.5, DHRS6 oxidizes (R)-OH butyrate with a $V_{\rm max}$ of 31.9 nmol \times min $^{-1}$ \times mg $^{-1}$ and a K_m of 12.6 mM. The enzyme follows a Michaelis-Menten kinetic pattern (Fig. 1C), and no signs for allosteric behavior were observed. The enzyme is specific for NAD $^+$ and shows a K_m for this cofactor of 59.8 μ M (cf. Table 1).

Crystal Structure of Human DHRS6—Crystals obtained diffracted to a resolution of about 1.84 Å, and phases were calculated by molecular replacement (for data processing and refinement statistics, see Table 2). The crystallographic asymmetric unit of human DHRS6 consists of four monomers (A-D), four NAD+ molecules, four sulfate molecules, and 869 water molecules. The final model contains residues 1-246 of chain A, residues 2-246 of chain B, and residues 2-245 of chains C and D. A Ramachandran plot (Procheck) indicates that 92% of the residues are in the most favored regions, and the remaining 8% are in the additional allowed (7.5%) and generously allowed (0.5%) regions. The 245-residue core domain of human DHRS6 (without residues introduced through cloning) forms a single α/β domain typical of SDR enzymes (Fig. 3). The topology is based on the Rossmann fold, with a seven-stranded parallel β -sheet (β A- β G), which is sandwiched between three α -helices on each side ($\alpha B - \alpha G$) (Fig. 3B). Additional secondary structural elements are inserted between βF and αG and consist of two short helices ($\alpha FG1$ (residues $\text{Asp}^{182}\text{-Arg}^{191}\text{)}$ and αFG2 (residues $\text{Asn}^{194}\text{-Arg}^{205}\text{),}$ connected by a turn introduced through Arg¹⁹² and Gly¹⁹³. Furthermore,



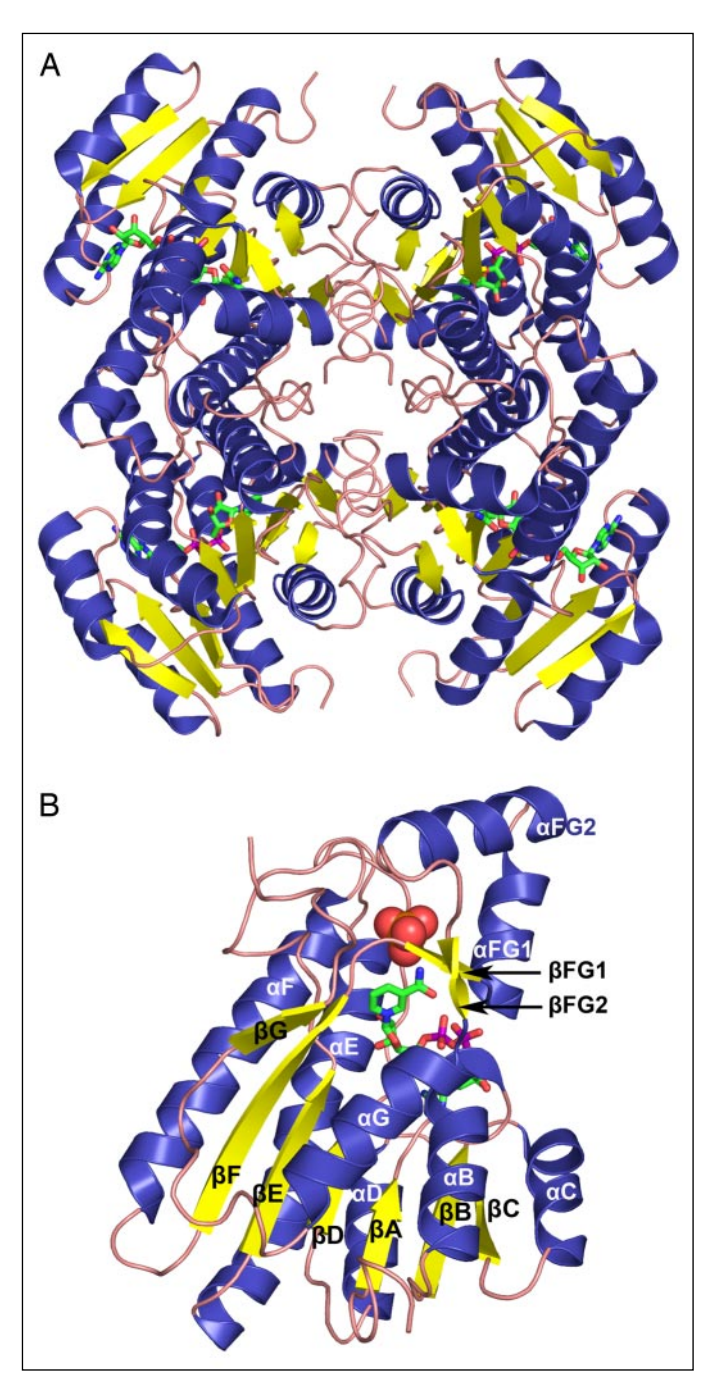


FIGURE 3. Overall structure of human DHRS6. A, tetrameric assembly of DHRS6 monomers with a 222-point group symmetry. B, ribbon diagram of a monomeric DHRS6 subunit, with NAD⁺ bound (presented as stick model; sulfate is shown in a sphere representation). The figure was generated using the program Pymol.

two short strands (β FG1 (Thr¹⁷⁹-Asp¹⁸¹) and β FG2 (Phe²¹¹-Thr²¹³)) preceding helices α FG1 and α G (Fig. 3C) are found. This region is the most dissimilar found in SDR enzymes and constitutes large parts of the substrate binding region (cf. Fig. 3C). Comparison of subunits of DHRS6 and rat type II hydroxyacyl-CoA dehydrogenase with bound NAD⁺ and acetoacetate (11) shows distinct secondary structure arrangements around the active site, despite conservation of catalytic residues.

The functional oligomeric state of the enzyme is a tetramer, composed of subunits A, B, C, and D, showing a 222-point group symmetry (Fig. 3A). DHRS6 thus displays a prototype quaternary arrangement as observed in several SDRs (e.g. bacterial $3\alpha/20\beta$ -HSD, rat type II HADH, or murine MLCR) (11-13).

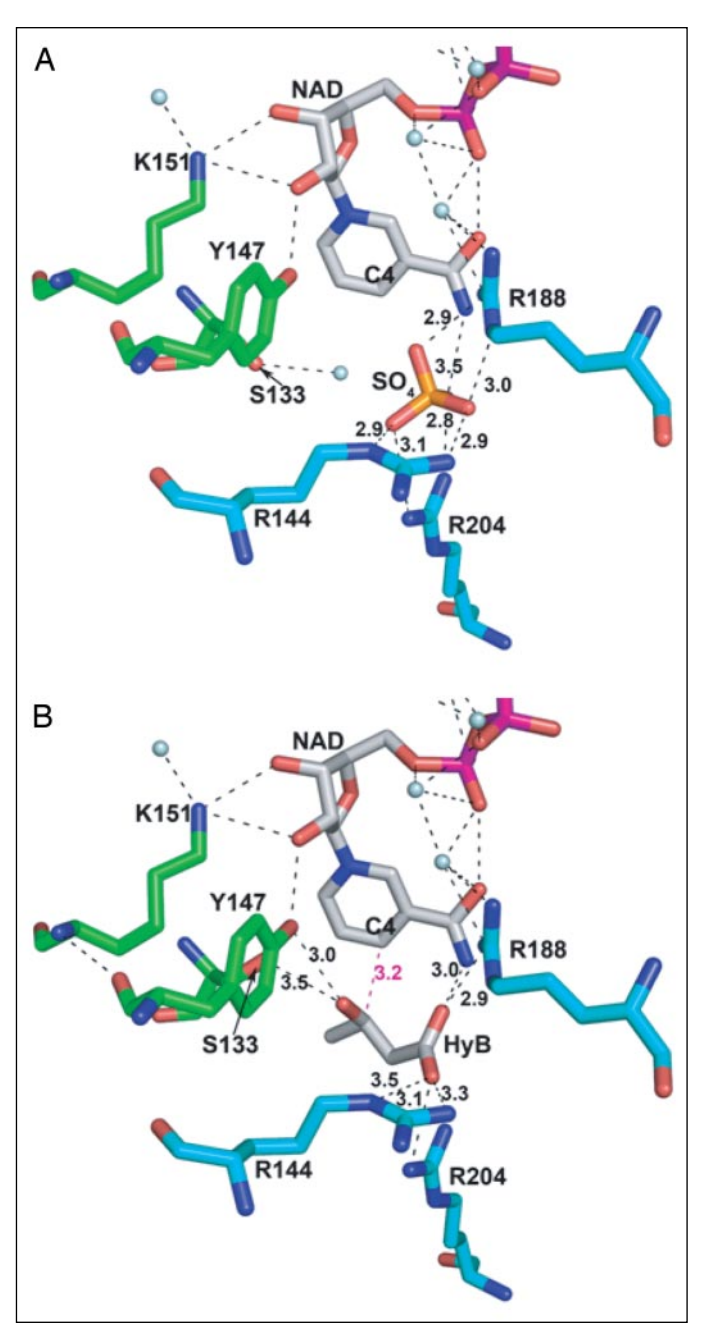


FIGURE 4. Active site of human DHRS6. A, the active site of DHRS6. The carbon atoms of the NAD cofactor are gray, the carbon atoms of the catalytic residues Ser^{133} , Tyr^{147} , and Lys^{151} are green, and carbon atoms of three arginines, Arg^{144} , Arg^{188} , and Arg^{205} , are cyan. The latter represent a highly conserved triple R motif, which in the crystal structure of DHRS6 is responsible for coordinating a sulfate ion (SO₄). Water molecules are depicted as pale blue spheres, and polar contacts are shown as dashed black lines. Some of the polar contact distances are shown in Ångstroms. B, the active site of DHRS6 following the in silico docking of the substrate (R)- β -hydroxybutyrate (HyB). The three conserved arginines, ${\rm Arg^{144}}$, ${\rm Arg^{188}}$, and Arg²⁰⁵, coordinate the carboxyl group of (R)-3-hydroxybutyrate, whereas the catalytic residues Ser¹³³ and Tyr¹⁴⁷ are interacting with the carbonyl group. The C3 hydrogen of (R)- β hydroxybutyrate is in close proximity (3.2 Å; shown as a magenta dashed line) and suitable orientation to facilitate hydride transfer to the C4 atom of the nicotinamide ring of the NAD+ cofactor. A and B were generated with the program Pymol.

Cofactor Binding and Active Site Architecture of Human DHRS6-The structure of DHRS6 was solved in complex with NAD⁺, and well defined electron density is observed for all parts of the cofactor molecule. NAD⁺ binds in an extended conformation (14.3 Å between C2 of nicotinamide and C6 of the adenine ring), with the adenine ring in anti conformation and syn for the nicotinamide ring, consistent with B-face



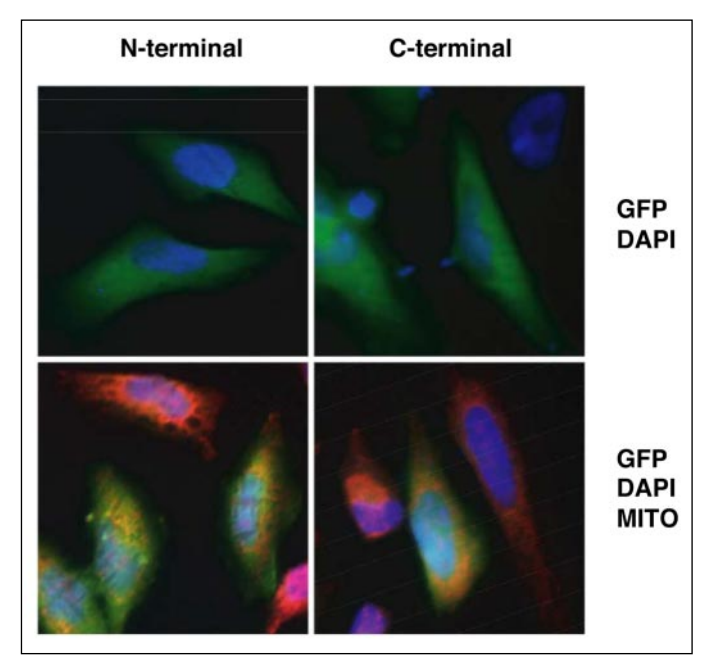


FIGURE 5. Subcellular localization of DHRS6 in HeLa cells. N- or C-terminal GFP fusion proteins localize to cytosol as indicated. The upper panels show fluorescence of GFP and staining of nuclei with 4'.6-diamidino-2-phenylindole (DAPI). The lower panels demonstrate lack of colocalization of DHRS6 with mitochondria (MITO).

4-pro-S hydride transfer. DHRS6 shows an unusual sequence motif (TAAAQGIG instead of TGXXXGIG found in the majority of SDRs), which determines the turn between βA and αB , necessary to accommodate the pyrophosphate moiety of the cofactor (6, 13, 14). The degree of variability in this basic and critical SDR motif is also observed in Drosophila ADH, which has the sequence VAALGIG (15).

The active site is a deep cleft, with the NAD⁺ cofactor forming the bottom of the active site cavity. The active site is flanked on one site by a long loop from Asn⁸⁰ to His⁸⁷, connecting etaD and lphaE, and on the other side by the loop connecting $\beta D-\alpha F$ and reaches further into helix αF (residues Ser¹³²-Lys¹⁵⁰). Within this cavity, the catalytic residues of DHRS6 are found at homologous positions previously identified in other SDR-type dehydrogenases (6, 16). These residues comprise Ser¹³³, Tyr¹⁴⁷, and Lys¹⁵¹ (Fig. 4A). Furthermore, the characteristic polar contacts between Tyr147, Lys151, the 2'- and 3'-OH of the nicotinamide, and the water contacts involving the main chain carbonyl of conserved Asn¹⁰⁵ and the side chain of Lys¹⁵¹, indicate a possible proton relay (16) (data not shown). The side chain of Asn¹⁰⁵ binds to the main chain amide of Phe⁸⁴, thus introducing a characteristic kink in helix αE , a structural motif found in the majority of SDR structures determined to date (16). Within the active site, a sulfate molecule derived from the crystallization solution, forms hydrogen bonds with the basic residues Arg¹⁴⁴, Arg¹⁸⁸, and Arg²⁰⁵ (Fig. 4A). These residues are found to be highly conserved in the DHRS6 cluster as well as the bacterial BDHs identified above (Fig. 1A). This suggests a conserved binding mode of this "triple R" motif to a negatively charged substrate group. The interaction described presumably closes the active site, by moving helices α FG1 (contacts between Arg¹⁸⁸-SO₄: 2.9 and 3.0 Å) and α FG2 (contacts between Arg^{205} - SO_4 : 3.1 and 2.8 Å) toward helix αF (contacts between Arg¹⁴⁴-SO₄: 2.9 and 2.9 Å) (Fig. 4A). Substrate docking of hydroxybutyrate into the active site of human DHRS6 was performed. The results generated by the docking protocol were then analyzed, and we present here the best solution satisfying the catalysis conditions. The three conserved arginines (Arg¹⁸⁸, Arg¹⁴⁴, and Arg²⁰⁵) are coordinating the carboxyl group of (R)-3-hydroxybutyrate, whereas the catalytic residues

Ser¹³³ and Tyr¹⁴⁷ are interacting with the carbonyl group. This results in the positioning of the C3-S hydrogen of (R)-hydroxybutyrate facing toward the nicotinamide ring of the cofactor, in close proximity (3.2 Å) for its transfer to the position C4 of NAD⁺ (Fig. 4B).

Subcellular Localization of Human DHRS6—Reporter experiments with either N- or C-terminally GFP-tagged human DHRS6 transfected into HeLa cells reveal a fluorescence pattern consistent with a cytoplasmic localization (Fig. 5). Moreover, no mitochondrial (Fig. 5) or endoplasmic reticulum (data not shown) targeting is observed using mitochondrial fluorescence dyes as reporter, thus distinguishing DHRS6 further from type 1 BDH.

DISCUSSION

Human DHRS6 and its vertebrate orthologs represent a striking example of structural and functional conservation between pro- and eukaryotic species. The high degree of sequence conservation and the confirmed overlapping substrate specificities between prokaryotic BDHs and human DHRS6 allow us to predict that prokaryotic members of this DHRS6/BDH cluster share significant structural similarities, as observed and discussed in the structure presented in this report. The similarities observed are not only found in the regular SDR sequence motifs defined earlier (6, 9, 16, 17) but also extend especially into the substrate and active site region, pointing to essentially the same substrate specificities and mechanisms. The enzymes described in this report are thus clearly different from mammalian type 1 (mitochondrial) BDH (sharing about 20% sequence identities), mammalian 3-hydroxyisobutyrate dehydrogenases involved in valine catabolism (18, 19) (sharing about 15% sequence identities), or the unrelated plant hydroxybutyrate dehydrogenases (20).

The high level of conservation in the DHRS6/BDH cluster also points to the essential role of 3-hydroxybutyrate as nutrient or building block in cellular survival, seemingly conserved during evolution. Importantly, in many bacterial species, energy and carbon sources are stored in the form of polyhydroxybutyrate, which can be mobilized into R-3-hydroxybutyrate and subsequently is converted into acetoacetate and acetyl-CoA, which then is directed into the tricarboxylic acid cycle (21). The bacterial BDHs play an essential role in this pathway, since 3-hydroxybutyrate needs to be converted into acetoacetate for further metabolism. Thus, 3-hydroxybutyrate is a universal, highly reduced carrier of cellular energy, since a similar role for this pathway has apparently evolved in mammals, where stored energy in lipids is mobilized through B-oxidation and conversion into acetoacetate and R-3-hydroxybutyrate. These ketone bodies are subsequently distributed into peripheral tissues that utilize it by conversion into acetyl-CoA.

Under our assay conditions, DHRS6 displays a fairly low turnover number. It is at this stage not possible to determine whether this low $k_{\rm cat}$ is due to any suboptimal conditions chosen in the in vitro characterization or if there are further, unknown regulatory factors important for activity, as observed, for example, with lipid dependence of the type 1 BDH enzyme. No information is currently available on the DHRS6related bacterial enzymes in regard to kinetic values. Certainly, the possibility exists that we have overlooked possible physiological substrates by using our narrow substrate screening. However, inspection of the active site of DHRS6 reveals a compact ligand pocket size, which is probably not suited to accommodate larger chain lengths than C4 of fatty acid acyl moieties. A substructure search using the determinants of a carboxylate and a 3-OH/oxo group reveal no relevant hits from the KEGG ligand data base (available on the World Wide Web at www.genome.ad.jp/kegg) other than the substrates tested. In the absence of other bona fide ligands, (R)-OH butyrate thus remains as a



cemic states or in disorders related to fatty acid and cholesterol synthesis.

Taken together, we have characterized a highly conserved member and cluster of the SDR family and show evidence of a possible functional role in mammalian physiology. Further studies in our laboratories are under way to investigate further the postulated role of DHRS6 in cellular models.

Acknowledgments—Fruitful discussions with Johannes Zschocke (University of Heidelberg) and Jorn Oliver Sass (University of Freiburg) are gratefully acknowledged. We are grateful to Brian Marsden (Structural Genomics Consortium) for performing the substructure data base search.

Note Added in Proof-The human DHRS6 gene has been officially approved by the Human Genome Nomenclature Committee (HGNC) as R-hydroxybutyrate dehydrogenase type 2 with the gene symbol BDH2 based on this publication.

REFERENCES

- 1. Chelius, D., Loeb-Hennard, C., Fleischer, S., McIntyre, J. O., Marks, A. R., De, S., Hahn, S., Jehl, M. M., Moeller, J., Philipp, R., Wise, J. G., and Trommer, W. E. (2000) Biochemistry 39, 9687-9697
- 2. Churchill, P., Hempel, J., Romovacek, H., Zhang, W. W., Brennan, M., and Churchill, S. (1992) Biochemistry 31, 3793-3799
- 3. Dalton, L. A., McIntyre, J. O., and Fleischer, S. (1993) Biochem. J. 296, 563-569
- 4. Green, D., Marks, A. R., Fleischer, S., and McIntyre, J. O. (1996) Biochemistry 35, 8158 - 8165
- 5. Marks, A. R., McIntyre, J. O., Duncan, T. M., Erdjument-Bromage, H., Tempst, P., and Fleischer, S. (1992) I. Biol. Chem. 267, 15459-15463
- 6. Jornvall, H., Persson, B., Krook, M., Atrian, S., Gonzalez-Duarte, R., Jeffery, J., and Ghosh, D. (1995) Biochemistry 34, 6003-6013
- 7. Kallberg, Y., Oppermann, U., Jornvall, H., and Persson, B. (2002) Protein Sci. 11, 636 - 641
- 8. Oppermann, U., Filling, C., Hult, M., Shafqat, N., Wu, X., Lindh, M., Shafqat, J., Nordling, E., Kallberg, Y., Persson, B., and Jornvall, H. (2003) Chem. Biol. Interact. 143, 247-253
- 9. Oppermann, U. C., Filling, C., and Jornvall, H. (2001) Chem. Biol. Interact. 130, 699 - 705
- 10. Totrov, M., and Abagyan, R. (1997) Proteins, Suppl. 1, 215-220
- 11. Powell, A. J., Read, J. A., Banfield, M. J., Gunn-Moore, F., Yan, S. D., Lustbader, J., Stern, A. R., Stern, D. M., and Brady, R. L. (2000) J. Mol. Biol. 303, 311-327
- 12. Ghosh, D., Weeks, C. M., Grochulski, P., Duax, W. L., Erman, M., Rimsay, R. L., and Orr, J. C. (1991) Proc. Natl. Acad. Sci. U. S. A. 88, 10064-10068
- 13. Tanaka, N., Nonaka, T., Nakanishi, M., Deyashiki, Y., Hara, A., and Mitsui, Y. (1996) Structure 4, 33-45
- 14. Ghosh, D., Wawrzak, Z., Weeks, C. M., Duax, W. L., and Erman, M. (1994) Structure 2.629 - 640
- 15. Benach, J., Atrian, S., Gonzalez-Duarte, R., and Ladenstein, R. (1999) J. Mol. Biol. 289, 335-355
- 16. Filling, C., Berndt, K. D., Benach, J., Knapp, S., Prozorovski, T., Nordling, E., Ladenstein, R., Jornvall, H., and Oppermann, U. (2002) J. Biol. Chem. 277, 25677-25684
- 17. Oppermann, U. C., Filling, C., Berndt, K. D., Persson, B., Benach, J., Ladenstein, R., and Jornvall, H. (1997) Biochemistry 36, 34-40
- 18. Hawes, J. W., Crabb, D. W., Chan, R. J., Rougraff, P. M., Paxton, R., and Harris, R. A. (2000) Methods Enzymol. 324, 218-228
- 19. Hawes, J. W., Harper, E. T., Crabb, D. W., and Harris, R. A. (1997) Adv. Exp. Med. Biol.
- 20. Breitkreuz, K. E., Allan, W. L., Van Cauwenberghe, O. R., Jakobs, C., Talibi, D., Andre, B., and Shelp, B. J. (2003) J. Biol. Chem. 278, 41552-41556
- 21. Aneja, P., and Charles, T. C. (1999) J. Bacteriol. 181, 849 857
- 22. Endemann, G., Goetz, P. G., Edmond, J., and Brunengraber, H. (1982) J. Biol. Chem. **257**, 3434 – 3440
- 23. Ohnuki, M., Takahashi, N., Yamasaki, M., and Fukui, T. (2005) Biochim. Biophys. Acta 1729, 147-153
- 24. Koundakjian, P. P., and Snoswell, A. M. (1970) Biochem. J. 119, 49-57
- 25. Leblanc, P. J., and Ballantyne, J. S. (2000) J. Exp. Zool. 286, 434-439

promoter region that are involved in lipid metabolism like retinoic acid receptor-responsive elements or nuclear factor Y binding motifs. Although mammalian or vertebrate BDH is almost exclusively discussed as mitochondrial (1, 5), this study and earlier reports (24, 25) present compelling evidence of a cytosolic type II BDH. In an earlier study, Koundakjian and Snoswell (24) noted a pronounced species difference in subcellular localization and organ distribution between cytosolic and mitochondrial BDH activity. Similarly, a complex subcellular and distribution pattern of teleost BDH was noted more recently (25), again pointing to a more complex BDH isozyme system. These data make it conceivable that humans and other vertebrates possess a cytosolic BDH, which is likely to be DHRS6, as deduced from the data of this study. DHRS6 is mainly expressed in the central nervous system and kidney, but also in heart and skeletal muscle, tissues that are highly dependent on sufficient fatty acid and energy supply. Importantly, the brain is able to switch its energy supply from glucose, under normal metabolic conditions, to ketone bodies as a supplemental energy source, reaching an estimated 50% of energy supply from this source.

physiological substrate. Accordingly, DHRS6 could play an important

role in the peripheral utilization of 3-hydroxybutyrate, based on the

following line of evidence. The cytoplasmic localization with its high

ratio of oxidized NAD⁺, the NAD⁺ dependence, and the kinetic param-

eters of DHRS6 make it suitable to convert high levels of circulating

3-hydroxybutyrate into acetoacetate. Comparison of kinetic parameters between recombinant mitochondrial BDH and type II BDH/DHRS6

shows that DHRS6 has a 2-3-order of magnitude lower catalytic spec-

ificity toward R-3-hydroxybutyrate (1, 4). However, the determined K_m

of about 10 mm makes DHRS6 suitable to function under high circulat-

ing levels of R-3-hydroxybutyrate, which are indeed found under pro-

longed starvation or in diabetic ketoacidosis. Furthermore, cytosolic levels of NAD⁺ are high, allowing efficient conversion into acetoacetate,

which can subsequently enter mitochondria and the tricarboxylic acid

cycle. This points to a possible role of DHRS6 as "backup" or lower

affinity system for utilization of hydroxybutyrate, with the type I BDH

working as the main system, localized to mitochondria. A different role

of cytosolic ketone body utilization might be the cytosolic generation of

acetoacetyl-CoA as building block for fatty acid and sterol synthesis,

independent from mitochondrial citrate supply (22). This is supported

by the demonstration of a cytosolic acetoacetyl synthetase (23), effi-

ciently converting acetoacetate into acetoacetyl-CoA, further incorpo-

rated into lipids (22). DHRS6 acts in this pathway to secure sufficient

amounts of cytosolic acetoacetate. In line with this observation is the

occurrence of transcription factor binding sites in the human DHRS6

The genomic organization of DHRS6 deduced from data deposited in public data bases reveals a 20.4-kbp gene organized in 10 exons. The DHRS6L gene located on chromosome 6q16.3 appears to be a pseudogene, further validated by the fact that it cannot be functionally expressed. DHRS6L lacks the C-terminal 11 residues found in DHRS6, and importantly this segment contains the eta G strand of the basic SDR/ Rossmann fold scaffold. Thus far, no single nucleotide polymorphisms or functional mutations have been identified within the DHRS6 gene, which is located on chromosome 4q24. All single nucleotide polymorphisms reported lie outside the coding region. According to the function described for DHRS6 in this study, deficiencies of DHRS6 might manifest in ketone utilization disorders, such as hyperketotic hypogly-



Characterization of Human DHRS6, an Orphan Short Chain Dehydrogenase/Reductase Enzyme: A NOVEL, CYTOSOLIC TYPE 2 R- β -HYDROXYBUTYRATE DEHYDROGENASE

Kunde Guo, Petra Lukacik, Evangelos Papagrigoriou, Marc Meier, Wen Hwa Lee, Jerzy Adamski and Udo Oppermann

J. Biol. Chem. 2006, 281:10291-10297. doi: 10.1074/jbc.M511346200 originally published online December 27, 2005

Access the most updated version of this article at doi: 10.1074/jbc.M511346200

Alerts:

- When this article is cited
- · When a correction for this article is posted

Click here to choose from all of JBC's e-mail alerts

This article cites 21 references, 7 of which can be accessed free at http://www.jbc.org/content/281/15/10291.full.html#ref-list-1